Beam Pattern Optimization for Integrated Sensing and Communication in UAV Applications

Juan A. Vásquez-Peralvo*, Gianluca Fontanesi*, Anna Guerra‡, Francesco Guidi§, Nir Shlezinger¶, Alberto Zanella§, Eva Lagunas*, Symeon Chatzinotas*, Davide Dardari‡, and Petar M. Djurić‖
* Interdisciplinary Centre for Security Reliability and Trust, University of Luxembourg, Luxembourg-
(e-mail: { juan.vasquez, eva.lagunas, symeon.chatzinotas}@uni.lu).
(e-mail: gianluca.fontanesi@ieee.org).
‡ Wilab, DEI, University of Bologna, Italy (e-mail: anna.guerra,davide.dardari@unibo.it).
§ National Research Council of Italy (e-mails: { francesco.guidi, alberto.zanella}@cnr.it).
¶ Ben Gurion University, Israel. (e-mail: irshl@bgu.ac.il).
‖ Stony Brook University, New York, USA (e-mail: petar.djuric@stonybrook.edu).

***Abstract*—The deployment of unmanned aerial vehicles (UAVs) equipped with uniform rectangular array (URA) offers a promising solution for simultaneous communication with multiple ground base stations (GBSs) and the sensing of ground-based target. However, designing a transmit beamforming system that optimizes communication while maintaining high sensing accuracy is challenging. In this regard, this paper proposes a comprehensive beam pattern optimization framework tailored for integrated sensing and communication in UAV applications, where the beam is synthesized based on the required steering direction, beamwidth, side lobe suppression, and nulling in targeted areas, providing robust connectivity. This comprehensive framework integrates sensing and communication, improving system performance and connectivity in UAV applications.**

***Index Terms*—Uniform Rectangular Array, phased arrays, genetic algorithm.**

I. Introduction

The integration of sensing and communication functions in unmanned aerial vehicles (UAVs) is becoming increasingly crucial for modern applications, ranging from surveillance and environmental monitoring to autonomous navigation, emergency response and even measurement antenna applications [1]. Equipped with advanced communication systems and sensors, UAVs must operate efficiently in complex environments, maintaining reliable communication links with ground stations and other airborne nodes while avoiding interference from signals coming from the ground or even from other UAVs [2]. One of the key challenges in these systems is the optimisation of the antenna beam pattern to simultaneously ensure high quality communications, precise sensing capabilities and interference mitigation, while taking into account the self-interference of the metallic components of the UAV [3].

Beam pattern optimization plays a pivotal role in enhancing both the sensing accuracy and communication reliability of UAVs. By dynamically adjusting the beam patterns, UAVs can mitigate interference, improve signal-to-noise ratios, and ensure broader or more focused coverage as required by the mission [4]. In addition, a proper beam optimization allows a better power management which is a very important aspect in this type of application. Moreover, with the advent of Integrated Sensing and Communication (ISAC) systems, the demand for joint optimization of these two functionalities has become more pronounced. In such systems, the same hardware is often used for both radar-based sensing and wireless communication, making beam pattern design a critical factor in achieving optimal performance for both tasks.

Recent works have proposed different approaches to improve the communications form UAV ranging from the optimisation of antenna arrays installed on non-conductive unmanned aerial vehicle [3], machine learning for beam tracking and weight optimization [4], beam search algorithm for anti-collision trajectory planning [5] and, finally, use of predictive beamforming framework based on a dual deep neural network (DNN) solution to find the optimum beamforming weights for a joint communication and sensing problem [6].

However, previous work lacks a comprehensive investigation of a beampattern optimization framework for a joint communication and sensing problem to evaluate its effectiveness in a UAV-based communication network scenario. In this paper, we demonstrate through simulations that a well-optimised beampattern is able to provide accurate beampattern and sensing performance.

II. System Model

We consider a cellular system composed of a terrestrial network of ground base stations (GBSs) and a single UAV equipped with an antenna array. The UAV simultaneously performs monostatic radar sensing of its surrounding environment while maintaining communication with an associated GBS. We assume that the UAV has access to all necessary information to select the most appropriate GBS for communication.

The signal transmitted by the UAV may cause interference to other nearby GBSs. For this reason, the communication and sensing performance has to be optimized by selecting an appropriate beam-pattern configuration for the UAV, using an ad-hoc beam-pattern optimization technique. This approach ensures that the UAV meets both communication and sensing requirements.

A. System Geometry

We consider that the UAV aims to sense the presence of a target placed at a known location $\mathbf{u}_0 = (x_0, y_0, z_0)$. The location of the GBSs are fixed at $\mathbf{u}_k = (x_k, y_k, z_k), \quad k = 1, ..., K$ with K being the number of deployed GBSs, (x_k, y_k) denoting the location of the kth GBS and $z_k = h_{\text{BS}}, \forall k$. Differently from [6], here we focus our interest on investigating the capabilities of the beam-pattern optimizer, so we account only for one UAV position $\mathbf{q} = (x, y, z)$.

B. Transmitted Signal Model

Let $\mathbf{s}$ be a $(K+1)\times 1$ vector containing the UAV transmitted waveforms as

$$\mathbf{s} = [\underbrace{s_0}_{\text{Sensing}}, \underbrace{s_1, \dots, s_k, \dots, s_K}_{\text{Communication}}]^T, \tag{1}$$

where s_k represents the transmitted signal from the UAV to the k-th GBS , whereas s_0 represents the transmitted signal for sensing. The UAV is connected to a single GBS, and (1) reduces to $\mathbf{s} = [s_0, s_{\hat{k}}]^T \in \mathcal{C}^{2\times 1}$, where $\hat{k}$ is the chosen GBS at a certain time instant. Also, we consider the UAV applying beamforming techniques for communications and sensing. We denote with $\mathbf{W}$ the beamforming matrix given by

$$\mathbf{W} = [\underbrace{\mathbf{w}_0}_{\text{Sensing}}, \underbrace{\mathbf{w}_{\hat{k}}}_{\text{Comm.}}] \in \mathcal{C}^{M\times 2} \tag{2}$$

with $\mathbf{w}_{\hat{k}} \in \mathcal{C}^{M\times 1}$ representing the corresponding transmit beamforming vector to the GBS, whereas $\mathbf{w}_0$ is the beamforming vector used for sensing. Thus, the ith beamforming vector, with $i \in \mathcal{I} = \{0, \hat{k}\}$, can be expressed as

$$\mathbf{w}_i = [\alpha_0 e^{\jmath\varphi_{i,0}}, \dots, \alpha_m e^{\jmath\varphi_{i,m}}, \dots, \alpha_{M-1} e^{\jmath\varphi_{i,M-1}}]^T \in \mathcal{C}^{M\times 1}, \tag{3}$$

where α_m is the mth antenna amplitude scaling factor, $\varphi_{i,m}$ is the phase at the m-th antenna of the UAV array and M is the total number of antennas. Accordingly, the overall transmitted signal from the UAV is given by

$$\mathbf{x}_{\hat{k}} = \mathbf{w}_0 s_0 + \mathbf{w}_{\hat{k}} s_{\hat{k}}, \tag{4}$$

where, according to [6], the constraint on the maximum transmitted power is

$$\|\mathbf{w}_0\|^2 + \|\mathbf{w}_{\hat{k}}\|^2 \leq P_{\text{max}}. \tag{5}$$

We consider the antenna array on board of the UAV operates in the THz frequency bands, that offer large available bandwidth for the communication and sensing needs. Due to space limitation, we omit here the details of the THz propagation characteristics and channel model, and we refer to [6] for a more detailed description.

C. Received Signal Model

The steering vector $\mathbf{a}(\mathbf{q}, \mathbf{u}_i)$ towards the ith destination can be expressed as [7]

$$\mathbf{a}(\mathbf{q}, \mathbf{u}_i) = \left[e^{\jmath 2\pi f_c \tau_0}, \dots, e^{\jmath 2\pi f_c \tau_m}, \dots, e^{\jmath 2\pi f_c \tau_{M-1}}\right], \tag{6}$$

where f_c is the central frequency, τ_m the inter-antenna delay, which depends on the position $\mathbf{p}_m$ of the mth array antenna.

As a result, the channel vector between the UAV and the ith destination can be written as the following $M \times 1$ vector:

$$\mathbf{h}_i(\mathbf{q}, \mathbf{u}_i) = \sqrt{\mathsf{PL}_i}\, e^{\jmath 2\pi f_c \frac{d_i}{c}}\, \mathbf{a}(\mathbf{q}, \mathbf{u}_i), \tag{7}$$

where PL is the pathloss, d_i the distance to the target, and the received signal at the ith destination can be written as

$$y_i = \mathbf{h}_i^H(\mathbf{q}, \mathbf{u}_i)\mathbf{x}_i + \nu_i \in \mathcal{C}, \tag{8}$$

where $\nu_i(n)$ is the additive circular complex white Gaussian noise (AWGN) with variance σ^2.

Note that the time of arrival (TOA) between the mth antenna of the UAV and the ith destination is approximated as

$$\tau_{m,i} \approx \tau_m + \frac{\|\mathbf{u}_i - \mathbf{q}\|}{c}, \tag{9}$$

where c is the speed of light and τ_m is the propagation time from the mth antenna to the array center located in $\mathbf{q}$.

Finally, for communication purposes, we consider the elevation and azimuth angles between the transmitter (UAV) and the receiver (GBS) as

$$\theta = \text{acos}\left(\frac{z - z_i}{d_i}\right), \quad \phi = \text{atan}\left(\frac{y - y_i}{x - x_i}\right), \tag{10}$$

with $d_i = \|\mathbf{u}_i - \mathbf{q}\|$.

Note that the UAV can adapt its beamforming weights and orientation according to communication and sensing needs.

III. Problem Formulation

This section illustrates the joint optimization problem to balance and find a trade-off between communication and sensor needs. Before presenting the problem, we separately introduce the metrics to be optimized for both functionalities.

a) Communication metric: For enhancing the communications between the UAV and the selected GBS, we consider the Signal-to-Noise-plus-Interference Ratio (SINR) at the $\hat{k}$-th GBS formulated as

$$\mathsf{SINR}(\mathbf{q}, \mathbf{u}_{\hat{k}}) = \frac{|\mathbf{h}_{\hat{k}}^H(\mathbf{q}, \mathbf{u}_{\hat{k}})\mathbf{w}_{\hat{k}}|^2}{\sigma^2 + |\mathbf{h}_0^H(\mathbf{q}, \mathbf{u}_0)\mathbf{w}_0|^2}. \tag{11}$$

We have considered the worst-case scenario where the receiver cannot cancel the radar signals' interference before decoding its desirable information signal [8].

b) Sensing metric: A key performance metric adopted in literature for radar signal design is the transmit beam-pattern [9], [10]. The transmit beam pattern describes the transmit signal power towards the target of interest. Without prior knowledge of the target location, the transmit signal power is pointed at any value in the range $[-\pi/2, \pi/2]$ to perform a target search in any direction. Here, we assume the target is fixed in one position and that the position is known a priori. In the following, we note the estimated position of the target as $\hat{\mathbf{u}}_0$.

Starting from [10], we can formalize the transmit beam-pattern gain towards location $\mathbf{u}_0$ as

$$B(\mathbf{q}, \mathbf{u}_0) = (\mathbf{a}(\mathbf{q}, \mathbf{u}_0))^H (\|\mathbf{w}_0\|^2 + \|\mathbf{w}_{\hat{k}}\|^2)\mathbf{a}(\mathbf{q}, \mathbf{u}_0). \quad (12)$$

We highlight that $\mathbf{a}(\mathbf{q}, \mathbf{u}_0)$ is a known function of θ, defined in (6).

Then, let $B^\star(\mathbf{q}, \mathbf{u}_i)$ denote the desired beam pattern, which specifies the desired beamforming weights and direction. We can then formalize a cost function C that defines the beam-pattern matching error as

$$C(\mathbf{q}, \mathbf{W}) = |B^\star(\mathbf{q}, \mathbf{u}_0) - B(\mathbf{q}, \mathbf{u}_0)|^2. \quad (13)$$

We note that, according to (12), we would like to find $\mathbf{W}$ under the total transmit power constraint such that the available transmit power is used to maximize the signal power at the locations of interest.

c) Problem formulation: Our objective is to minimize the beam-pattern gain error, expressed in (13) optimizing $\mathbf{W}$, subject to a connectivity constraint. Thus, our optimization problem can be formulated as

$$\begin{aligned} \mathcal{P} : \min_{\mathbf{W}, \hat{k}} \quad & C(\mathbf{q}, \mathbf{W}) && (14a) \\ \text{s.t.} \quad & z > z_{\hat{k}} = h_{\text{BS}}, && (14b) \\ & \|\mathbf{w}_0\|^2 + \|\mathbf{w}_{\hat{k}}\|^2 \leq P_{\text{max}}, && (14c) \\ & \mathsf{SINR}(\mathbf{q}, \mathbf{u}_{\hat{k}}) \geq \gamma_{\text{SINR}}. && (14d) \end{aligned}$$

where (14b) ensures the UAV height respects the local height regulations, with h_{BS} indicating the minimum required height. Then, (14c) denotes the power constraint on the UAV, with P_{max} denoting the maximum tolerable transmitted power. Finally, (14d) ensures the minimum connectivity constraint with the GBS.

IV. Antenna Design

Before going into the details of antenna design, we recall that the considered antenna array on board the UAV operates in the THz frequency bands. Consequently, conventional antennas like patch antennas are not suitable for use at such high frequencies [11]. Instead, we employ an open-ended waveguide since this type of antenna does not use any substrate, which will highly reduce the chance of losses. The general radiation pattern $\hat{\mathbf{E}}(r, \text{El}_0, \text{Az}_0)$ of the open-ended waveguide can be modeled according to

$$\hat{\mathbf{E}}(r, \text{El}_0, \text{Az}_0) = E_0 \frac{J_1 (k r_{\text{ap}} \sin \text{El}_0)}{k r_{\text{ap}} \sin \text{El}_0} \frac{e^{-jkr}}{r} \left(\cos(\text{Az}_0)\hat{\theta} + j \sin(\text{Az}_0)\hat{\phi}\right)$$

where E_0 is the amplitude scaling factor, J_1 represents the Bessel function of first order, $k = \frac{2\pi}{\lambda}$ is the wave number, r_{ap} denotes the radius of the waveguide, r indicates the distance from the waveguide's aperture, El_0 and Az_0 are the elevation and azimuthal angles, $\hat{\theta}$ and $\hat{\phi}$ are unit vectors in the polar and azimuthal directions.

Finally, we configure the phased array antenna to provide full control over the amplitude and phase contribution of each antenna element. This allows us to perform phase synthesis to steer the beam in desired directions in azimuth and elevation (as defined in Eq. 10 respectively) and create nulls in others. This flexibility also enables tapering control, allowing for precise management of the transmitted power, side lobe level (SLL), and beamwidth.

V. Beamforming algorithm based on Demand

First, we note that (14) can be considered as a beamforming design problem. To control the constraints in (14) while finding the beamforming matrix, we consider a beam-pattern optimizer [12], that lets us manage the different requirements of the beamforming applied at the UAV. We consider a realistic antenna and a realistic number of antenna elements to perform the communication and sensing task and compute the inherent footprint. Second, the direction angle, measured in azimuth and elevation, is geometrically defined by the position of the UAV, of the associated GBS and of the target. According to the aforementioned considerations, the nulling operation has to be performed in the directions of the non-attached GBSs. Accordingly, we consider a opend-ended waveguide that generates a cardioid radiation pattern and a maximum number of $M = 100$ elements. The beamwidth is controlled by deactivating and tapering rows and columns of the matrix associated with the antenna array. This means that besides applying a Chebyshev tapering the algorithm will deactivate entire rows and columns. Then, the SLL constraint is addressed by tapering a fair number of active elements, and, finally, the EIRP is also estimated based on the variation of the antenna gain.

The radiation pattern optimiser works by enabling or disabling the number of active rows (m_x) and columns (m_z) in the array and finding the correct taper by selecting the appropriate SLL in both planes to generate the required $\theta_{3\text{dB}}$ in the elevation ($\theta_{3\text{dB}}^{(\text{e})}$) and azimuth ($\theta_{3\text{dB}}^{(\text{a})}$) planes, and calculating the required power per element to address the required effective isotropic radiated power (EIRP). For the position of the UAV, both the sensor and the communication array weight vectors are computed.

According to the previous considerations, the cost function is composed of the sum of two sub-objectives as follows

$$\mathbf{W}_{gv}^{\star} = \min_{\mathbf{W}_{gv}} \quad Z_1(\mathbf{W}_{gv}) + Z_2(\mathbf{W}_{gv}), \tag{15}$$

where $\mathbf{W}_{gv}$ indicates the gv-th element of the beamforming matrix, with

$$\begin{cases} Z_1(\mathbf{W}_{gv}) = \left(\frac{|\mathrm{SLL}_{\mathrm{c}}^{(\mathrm{Az})}(\mathbf{W}_{gv}) - \mathrm{SLL}_{\mathrm{o}}^{(\mathrm{Az})}|}{\mathrm{SLL}_{\mathrm{o}}^{(\mathrm{Az})}} \right. \\ \qquad \left. + \frac{|\mathrm{SLL}_{\mathrm{c}}^{(\mathrm{El})}(\mathbf{W}_{gv}) - \mathrm{SLL}_{\mathrm{o}}^{(\mathrm{El})}|}{\mathrm{SLL}_{\mathrm{o}}^{(\mathrm{El})}} \right) \cdot k_1 \\ Z_2(\mathbf{W}_{gv}) = \frac{\mathrm{EIRP}(\mathbf{W}_{gv}) - \mathrm{EIRP}^*}{\mathrm{EIRP}^*} \cdot k_2 \,. \end{cases} \tag{16}$$

with k_1 and k_2 being two weighting factors.

Note that $Z_1(\mathbf{W}_{gv})$ computes the error between the minimum desired SLL in both planes, that is, $\mathrm{SLL}_{\mathrm{o}}^{(\mathrm{Az})}, \mathrm{SLL}_{\mathrm{o}}^{(\mathrm{El})}$ compared to their computed counterparts $\mathrm{SLL}_{\mathrm{c}}^{(\mathrm{Az})}, \mathrm{SLL}_{\mathrm{c}}^{(\mathrm{El})}$ per beam. $Z_2(\mathbf{W}_{gv})$ reports the error between the desired EIRP^* and the calculated EIRP per beam.

VI. Numerical Evaluation

In this paper, we select an antenna aperture of 0.58λ (with a radius $r_{\mathrm{ap}} = 0.29\lambda$) and an inter-element spacing of 0.6λ. The total array spans a size of $6\lambda_0 \times 6\lambda_0$, such that it results in 10×10 antenna elements arranged in a square aperture with a rectangular lattice distribution.

To assess the performance of the proposed algorithm, we position the UAV at an altitude of 30 meters, with coordinates $(\varphi, \lambda) = (49°30'21.24''\,N, 6°8'15''\,E)$. The GBSs positions relative to the UAV are detailed in Tables I and II. Table I describes a non-challenging scenario where the sensing target and the connected GBS are close in terms of azimuth and elevation directions. Table II, instead, presents a more complex configuration. The shorter distances between GBS, in fact, increase the degree of complexity for the beampattern optimizer. Both scenarios are subject to additional constraints, including a minimum SLL greater than 18 dB and an EIRP of 18 dBm.

The resulting radiation patterns for the previous required beams are illustrated in Figure 3. For the first scenario, illustrated in Figure 3a (ISAC), 3b (Communication) , and 3c (Sensing), the algorithm performs well in synthesizing the beams due to the separation of the main beams. Additionally, the required nulling, where interference from other base stations is suppressed, is located in the correct positions. The SLL and EIRP requirements are successfully met for sensing, communications, and ISAC. The power allocation is also clearly identified by analyzing the amplitude contribution of the antennas illustrated in Figure 1.

Conversely, in the second scenario, the algorithm performs well in synthesizing the communication (Figure 3e) and sensing ((Figure 3f)) beams, but it encounters difficulties when synthesizing the required beam for the ISAC case (Figure 3d). One of the primary challenges is that the main beams are in close proximity, making it difficult to define a clear half-power beamwidth. This affects the SLL and EIRP, with the SLL reaching 16.23 dB and the EIRP reaching 22.45 dBm. The high EIRP results from the overlapping of the main beams, coming from the superposition of the amplitude contributions of the antennas in the direction where the main beams where pointing, as illustrated in Figure 2.

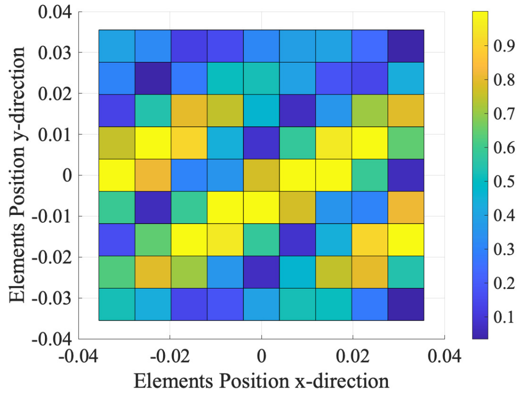

Fig. 1: Amplitude taper corresponding to the radiation pattern presented in Fig 3.

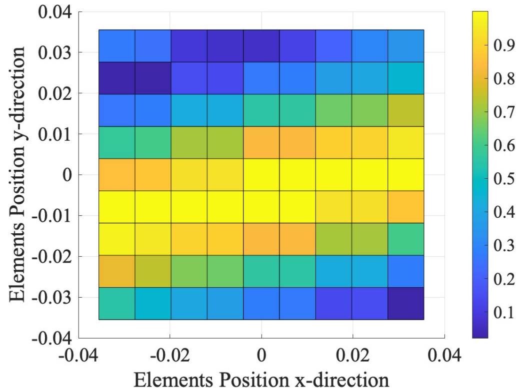

Fig. 2: Amplitude taper corresponding to the radiation pattern presented in Fig 3.

TABLE I: Configuration Parameters for Scenario 1.

Parameter	Communications Scenario	Sensing Scenario
(ϕ, θ)	(30°, -25°)	(0°, 0°)
$(\phi_{\mathrm{Null}_1}, \theta_{\mathrm{Null}_1})$	(30°, 25.02°)	——
$(\phi_{\mathrm{Null}_2}, \theta_{\mathrm{Null}_2})$	(-30.3°, -20.02°)	——

TABLE II: Configuration Parameters for Scenario 2.

Parameter	Communications Scenario	Sensing Scenario
(ϕ, θ)	(45°, -45°)	(30°, -30°)
$(\phi_{\mathrm{Null}_1}, \theta_{\mathrm{Null}_1})$	(30°, 25.02°)	——
$(\phi_{\mathrm{Null}_2}, \theta_{\mathrm{Null}_2})$	(-30.3°, -20.02°)	——

VII. Conclusion

In this paper, we have presented an algorithm that allows to compute the radiation pattern of an open-ended phase

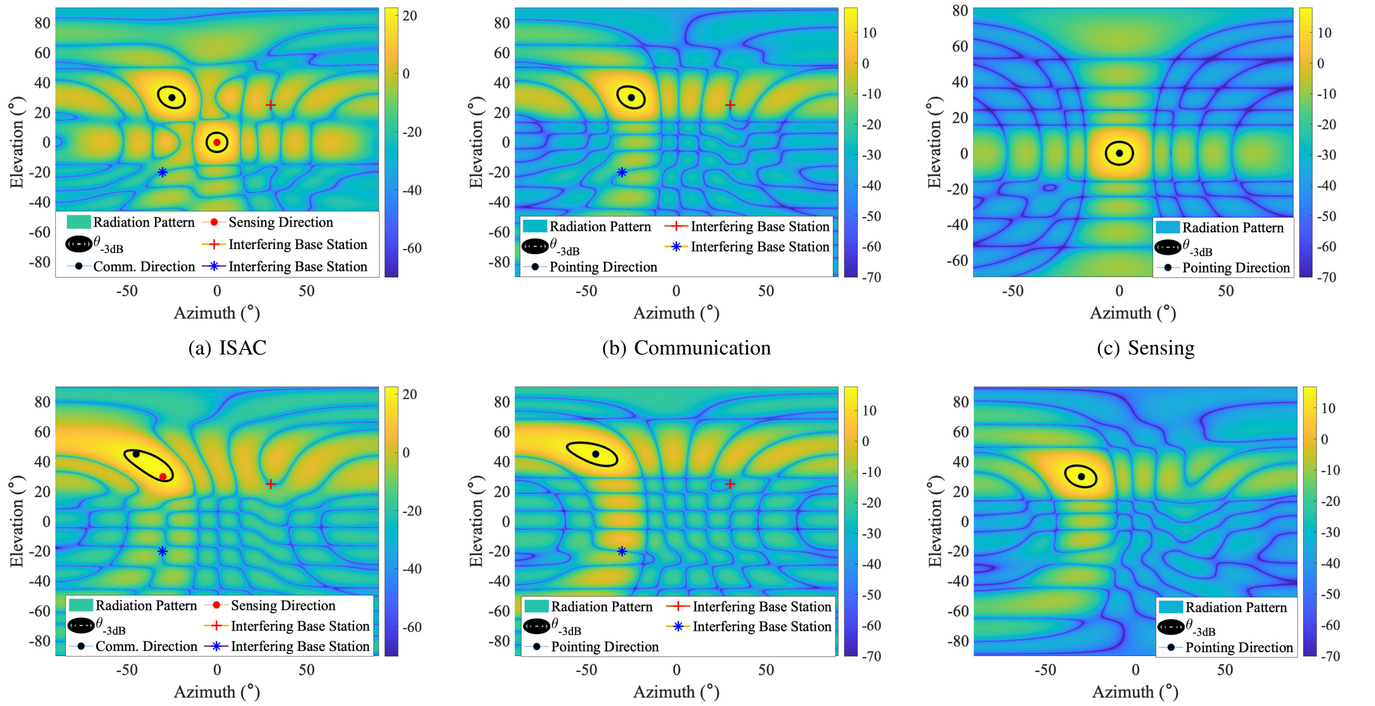

(a) ISAC (b) Communication (c) Sensing

(d) ISAC (e) Communication (f) Sensing

Fig. 3: Radiation patterns generated by the beam pattern optimizer for the scenarios in Table I and II. The unit of the colormap is dBm. The black circle indicates the main radiation HPBW lobe where most of the power is directed. The stars represent the positions of the neighbouring GBS.

array based on required inputs like desired SLL, main beam direction, required nulling directions, and target EIRP. The algorithm allowed us to perform the synthesization of the beams in three different scenarios, with requirements in terms of communication, sensing, and both (ISAC). For all the scenarios the synthesizing is achieved through the beamforming optimzer algorithm to reduce the activation on antenna elements as well as the surrogate algorithm to determine the desired antenna tapering.

ACKNOWLEDGMENT

This work has been supported by the European Space Agency (ESA) funded under Contract No. 4000134522/21/NL/FGL named "Satellite Signal Processing Techniques using a Commercial Off-The-Shelf AI Chipset (SPAICE)". Please note that the views of the authors of this paper do not necessarily reflect the views of ESA.

REFERENCES

[1] C. Sun, G. Fontanesi, B. Canberk *et al.*, "Advancing uav communications: A comprehensive survey of cutting-edge machine learning techniques," *IEEE Open Journal of Vehicular Technology*, 2024.

[2] A. Guerra, F. Guidi, D. Dardari, and P. M. Djurić, "Networks of UAVs of low complexity for time-critical localization," *IEEE Aerosp. Elect. Syst. Mag.*, vol. 37, no. 10, pp. 22–38, 2022.

[3] E. Yoshimoto, E. R. Schlosser, and M. V. T. Heckler, "Optimisation of antenna arrays installed on non-conductive unmanned aerial vehicle," *IET Microw., Ant. & Propag.*, vol. 12, no. 15, pp. 2292–2300, 2018.

[4] H.-L. Chiang, K.-C. Chen, W. Rave, M. Khalili Marandi, and G. Fettweis, "Machine-learning beam tracking and weight optimization for mmwave multi-uav links," *IEEE Transactions on Wireless Communications*, vol. 20, no. 8, pp. 5481–5494, 2021.

[5] J. Koszelew, J. Karbowska-Chilinska, K. Ostrowski *et al.*, "Beam search algorithm for anti-collision trajectory planning for many-to-many encounter situations with autonomous surface vehicles," *Sensors*, vol. 20, no. 15, p. 4115, 2020.

[6] G. Fontanesi, A. Guerra, F. Guidi *et al.*, "A deep-NN beamforming approach for dual function radar-communication THz UAV," *IEEE Trans. Veh. Technol.*, pp. 1–13, 2024.

[7] A. Guerra, F. Guidi, and D. Dardari, "Single-Anchor Localization and Orientation Performance Limits Using Massive Arrays: MIMO vs. Beamforming," *IEEE Trans. Wireless Commun.*, vol. 17, no. 8, pp. 5241–5255, 2018.

[8] H. Hua, J. Xu, and T. X. Han, "Optimal Transmit Beamforming for Integrated Sensing and Communication," *IEEE Trans. Veh. Technol.*, vol. 72, no. 8, pp. 10 588–10 603, 2023.

[9] D. R. Fuhrmann and G. San Antonio, "Transmit Beamforming for MIMO Radar Systems Using Signal Cross-Correlation," *IEEE Trans. Aerosp. Electron. Syst.*, vol. 44, no. 1, pp. 171–186, 2008.

[10] X. Liu, T. Huang, N. Shlezinger *et al.*, "Joint Transmit Beamforming for Multiuser MIMO Communications and MIMO Radar," *IEEE Trans. Signal Process.*, vol. 68, pp. 3929–3944, 2020.

[11] J. A. Vásquez-Peralvo, J. C. M. Duncan, V. Singh, G. Eappen, and S. Chatzinotas, "Drone-measurement-based antenna analysis: Multipath effects on radiation patterns," in *2024 IEEE International Symposium on Antennas and Propagation and INC/USNC-URSI Radio Science Meeting (AP-S/INC-USNC-URSI)*, 2024, pp. 1453–1454.

[12] J. A. Vásquez-Peralvo, J. Querol, F. Ortíz *et al.*, "Flexible beamforming for direct radiating arrays in satellite communications," *IEEE Access*, 2023.